Spatial and Time-Dependent Concentration Fluctuations of the Isobutyric Acid–Water System in the Neighborhood of Its Critical Mixing Point[1a]

B. Chu,[1b] F. J. Schoenes,[1c] and W. P. Kao

Contribution from the Chemistry Department, The University of Kansas, Lawrence, Kansas 66044. *Received November 20, 1967*

Abstract: The coexistence curve and critical opalescence of a binary liquid mixture, isobutyric acid–water, have been reinvestigated. Experiments are reported on the angular and the spectral distribution of scattered light for this system at critical solution concentration over a range of temperatures near the critical solution temperature in the one-phase region. The results are discussed in terms of the effects of long-range correlations. We observe that the temperature dependence of the extrapolated zero-angle scattered intensity obeys a relation $\lim_{K\to 0}(1/I_c^*) \propto (\partial\pi/\partial c)_T \propto (T - T_c)^{\gamma}$ with $\gamma \approx 5/4$, and that of the extrapolated line width from quasi-elastic scattering studies obeys a relation $\lim_{K\to 0} \Gamma/K^2 = \alpha^*(\partial\pi/\partial c)_T \propto (T - T_c)^{\gamma^*}$ with $\gamma^* = 2/3$. The rate at which the diffusion coefficient $D\,(=\alpha^*(\partial\pi/\partial c)_T)$ decreases in the neighborhood of the critical mixing point, as the temperature T approaches the critical solution temperature T_c, is therefore not entirely dictated by the decrease in the inverse susceptibility, $(\partial\pi/\partial c)_T \propto (T - T_c)^{\gamma}$. The discrepancy ($\gamma \neq \gamma^*$) implies that the transport coefficient α^* diverges as $(T - T_c)^{\gamma^*-\gamma}$ within the temperature range of our investigation.

In recent years many scientists have been interested in investigating the important and intriguing phenomena of second-order phase transitions. A cross section of current theoretical concepts and several ingenious experiments on studies dealing with critical points of liquid–vapor transitions, consolute points in binary fluid mixtures or alloys, Curie and Néel points in magnetism, λ points in liquid helium, and second-order phase transitions in solids can be found in the very informative proceedings of a conference on critical phenomena.[2] Experimental studies on the nature of correlation functions for systems undergoing phase transitions have been extensive ever since Debye published his theory on critical opalescence about 10 years ago.[3] Although initial efforts have been concentrated on studying the nature of isotropic three-dimensional spatial correlation functions by means of angular dissymmetry measurements,[2,4] recent developments on laser heterodyne[2,5] and "self-beating"[2,6] techniques permit us to study the form of space–time correlation functions. The angular and spectral distribution of scattered light remains one of the best and most direct ways of determining the correlation function. This approach is especially suitable for systems in the neighborhood of critical points because electromagnetic waves, with the exception of high power density focused laser beams, impose virtually no gradient upon the system. In addition, conventional measurements on thermodynamic and transport properties, such as isothermal compressibility and diffusion constant, become exceedingly difficult.

We should select systems consisting of simple spherical molecules, preferably a monatomic rare gas, and try to do our measurements very near the critical point if we want to compare our experiments with theory. Unfortunately, we have not been able to see our way clear on the effects of gravity[7] in critical opalescence studies of one-component systems. On the other hand, it is within reason to expect that the present-day techniques and the latest findings have been sophisticated enough so that decisive and meaningful measurements on one-component systems will be forthcoming in the near future. In the meantime, we have concentrated our efforts on the scattering behavior of two-component fluid mixtures where concentration fluctuations are predominant. It is interesting to note that the behavior of a binary liquid mixture which undergoes phase separation is, in many ways, closely analogous to the condensation of a simple fluid, and yet at the same time the molecular complexities of binary liquid mixtures may provide specific characteristics which vary from system to system. Hence, comparison between experiments and theory is usually more involved. Furthermore, we keep in mind that there are no binary liquid mixtures that possess all the desirable qualities capable of satisfying both the theorists and the experimentalists. The purpose of this article is to point out the salient points and some of the difficulties in critical opalescence and to examine critical opalescence of binary liquid mixtures using angular as well as spectral distribution of scattered light of the isobutyric acid–water system with refined techniques. We have reexamined the coexistence curve before we proceed with our "elastic" and quasi-elastic scattering experiments because it is important to specify the

(1) (a) This work was supported by the National Science Foundation and the Army Research Office, Durham; (b) Alfred P. Sloan Research Fellow; author to whom requests for reprints should be addressed; (c) on leave of absence from the University of Saarland, Saarbrücken, Germany.

(2) "Proceedings of a Conference on Critical Phenomena," National Bureau of Standards Miscellaneous Publication 273, M. S. Green and J. V. Sengers, Ed., U. S. Government Printing Office, Washington, D. C., 1966.

(3) P. Debye in "Non-Crystalline Solids," V. D. Frechette, Ed., John Wiley and Sons, Inc., New York, N. Y., 1960; *J. Chem. Phys.*, 31, 680 (1959); see also B. Chu, "Molecular Forces based on the Baker Lectures of Peter J. W. Debye," John Wiley and Sons, Inc., New York, N. Y., 1967.

(4) (a) See, for example, B. Chu, *J. Chem. Phys.*, 41, 226 (1964); (b) *J. Am. Chem. Soc.*, 86, 3557 (1964); (c) "Electromagnetic Scattering," R. L. Rowell and R. S. Stein, Ed., Gordon and Breach Science Publishers, New York, N. Y., 1967.

(5) H. Z. Cummins, N. Knable, and Y. Yeh, *Phys. Rev. Letters*, 12, 150 (1964); S. S. Alpert, Y. Yeh, and E. Lipworth, *ibid.*, 14, 486 (1965).

(6) N. C. Ford, Jr., and G. B. Benedek, *ibid.*, 15, 649 (1965).

(7) B. Chu and J. A. Duisman, *J. Chem. Phys.*, 46, 3267 (1967); B. Chu and R. J. Bearman, *ibid.*, in press.

thermodynamic state of the system. Our task also attempts to obtain the angular and spectral distribution of the scattered intensity (and their corresponding temperature dependence) over a large enough range and with sufficiently fine resolution so that we may have a more meaningful comparison between experiments and existing approximate theories.[3,8,9]

"Elastic" Scattering and Spatial Correlation Function. The scattered intensity $I(K)$ is related to the isotropic spatial correlation function[3] $C(r)$ with the form

$$I(K) \propto \int C(r) \frac{\sin Kr}{Kr} \, d\tau \qquad (1)$$

In this relation, $K = ks$, $k = 2\pi/\lambda$, λ being the wavelength of light in the medium, $s = 2 \sin(\theta/2)$, θ being the scattering angle between the incident beam and the direction of observation, and $d\tau$ is a volume element. For small values of K, we may write

$$\frac{I(K)}{I(0)} = 1 - \frac{K^2L^2}{6} + \cdots \qquad (2)$$

in which $I(0)$ is the scattered intensity for $K = 0$, and L is the Debye persistence length, defined as

$$L^2 = \int r^2 C(r) \, d\tau / \int C(r) \, d\tau$$

Equation 2 tells us that the scattered intensity becomes independent of the scattering angle θ as L approaches zero. Realizing that KL is a more appropriate variable, we may design our experiments with the following aims in mind. We want measurements (a) at small values of K in order to obtain the extrapolated zero-angle scattered intensity and to investigate *very* long-range correlations if they exist, (b) over large ranges of K in order to get more details on the shape of the correlation function, and (c) over an adequate temperature range so as to determine the temperature dependence of the extrapolated zero-angle scattered intensity and the decay of correlation function very near the critical point. Aim a can best be accomplished by means of conventional light scattering. The crucial question is how small a K do we have to reach before we can safely obtain the extrapolated zero-angle scattered intensity? There has been one report which shows a very steep scattering curve below 1° of angle using visible light.[10] This implies the presence of correlation lengths approaching macroscopic sizes which can perhaps be observed even with a magnifying lens! Our justifications in ignoring those findings are that, firstly, the reciprocal extrapolated zero-angle scattered intensity $I(0)^{-1}$ approaches zero as the temperature distance from the critical solution temperature $\Delta T = (T - T_c)$ approaches zero whenever the measurements have been done correctly. The fact that $\lim_{\Delta T \to 0} I(0)^{-1} \neq 0$ in many experiments can often be attributed to other experimental artifacts. Secondly, we have not been able to observe those macroscopic "droplets" with a magnifying lens. We shall assume that the *very* long-range correlations, if they exist, are important only in the very immediate neighborhood of the critical point. For this and other additional reasons to be discussed later, we have concentrated our investigation over fairly large temperature and angular ranges but have postponed the studies very close to the critical point and at scattering angles θ below 11°. Aim b requires the superimposition of angular measurements from scattering of visible light of various wavelengths as well as small angle scattering of X-rays.[4] Unfortunately, we have been unable to design a X-ray sample cell with materials inert to the isobutyric acid.[11] So, measurements on the small angle scattering of X-rays have to be delayed. The system isobutyric acid–water has a fairly strong opalescence which permits intensity and line-width studies to several degrees away from the critical solution temperature. It is a good choice for determining the temperature dependence of the extrapolated zero-angle scattered intensity. However, it is not suitable for studying the decay of correlation in the very immediate neighborhood of the critical mixing point because of multiple scattering with existing optics and geometry in our instrumentation.

Quasi-Elastic Scattering and Space–Time Correlation Function. For composition fluctuations in binary liquid mixtures, the relaxation is diffusion controlled.[12] The time-dependent correlation function for concentration fluctuations has the form

$$\langle \delta c(\vec{K},t + \tau) \delta c(\vec{K},t) \rangle = \langle |\delta c(\vec{K},t)|^2 \rangle e^{-\Gamma\tau} \qquad (3)$$

in which 2Γ is the half-width of a Lorentzian line centered at $\omega = 0$ if we use the "self-beating" technique of Benedek.[6] Fixman[9] and others have taken into account long-range correlation effects by relating the local osmotic pressure fluctuations to the amplitude as well as the gradient of concentration fluctuations so that the equation

$$\Gamma = DK^2(1 + K^2/\kappa^2) = (a + bK^2)K^2 = \alpha^* \left(\frac{\partial \pi}{\partial c}\right)_T K^2(1 + K^2/\kappa^2) \qquad (4)$$

has also a K^4 term. Here κ refers to the Ornstein–Zernike inverse correlation length with $G(r) \propto e^{-\kappa r}/r$, D is the "mutual diffusion coefficient," and α^* is the transport coefficient which relates the diffusion coefficient D ($\equiv a$) to the osmotic pressure gradient. We have indicated D as a binary diffusion coefficient. However, we are not certain how D should behave in the critical region. According to eq 4, we realize that it is important to measure the spectral distribution over a range of K and at various fixed temperature distances away from the critical mixing point. Our reasons for choosing the isobutyric acid–water system have been described elsewhere.[13] We may add that the extremely narrow line widths of this system in the very immediate neighborhood of the critical mixing point have again prevented us from studies in that range. However, as we have stated before, we want to utilize the large Debye molecular interaction parameter and a reasonably strong opalescent behavior to cover a large enough temperature range and to investigate the deviation from

(8) (a) M. E. Fisher, *J. Math. Phys.*, 5, 944 (1964); (b) R. D. Mountain, *Rev. Mod. Phys.*, 38, 205 (1966).

(9) M. Fixman, "Pontificae Academiae Scientiarum Scripta Varia 31—Study Week on the Molecular Forces, 18–23 April 1966," to be published.

(10) D. McIntyre, and A. M. Wims in ref 4c; see ref 26 of this footnote.

(11) Through joint efforts with P. W. Schmidt, Physics Department, University of Missouri, Columbia, Mo.

(12) P. Debye, *Phys. Rev. Letters*, 14, 783 (1965).

(13) B. Chu, *ibid.*, 18, 200 (1967).

the pure K^2 dependence in Γ, not in the very immediate neighborhood of the critical mixing point.

Experimental Section

We have paid particular attention to experimental details because of the many difficulties which one encounters in critical opalescence studies.

Materials. The materials used were purified as follows. Isobutyric acid (Fisher certified reagent grade) was purified by preparative gas chromatography using a 20 ft long × $^3/_8$ in. o.d. column packed with 30% FFAP on 60–80 Chromosorb P. The following conditions were used: column temperature 195°, injection temperature 190°, detector temperature 215°, time period for each cycle ≅27 min, injection volume ≅0.4–0.5 ml each time. Only a short cut in the main peak was collected under helium. The purified isobutyric acid was further fractionally distilled over active dried chromatographic alumina in a small vacuum distillation apparatus in order to eliminate dusts, water, and possibly small amounts of low-boiling-point solvents. We then checked the distilled isobutyric acid with (a) the same column used for purification and (b) a 6 ft long × 0.25 in. o.d. column packed with 80–120 Hewlett-Packard Polyaromatic Resin-1 (PAR-1). The estimated impurity was less than 0.01%. Deionized doubly distilled water[13] was again distilled in the same vacuum distillation apparatus in order to eliminate dusts and carbon dioxide.

Preparation of Solutions. The solutions were prepared in 10 cm × 10 mm o.d. selected Pyrex glass tubings by introducing each component separately with microsyringes over nitrogen atmosphere in a glove box. The precision microsyringes were calibrated to 0.0005 ml. Errors in concentration for each sample were estimated at less than 0.2%. The glass cells were then carefully and quickly sealed over a gas–oxygen flame. We prepared three sets of samples: one set used cells with Teflon stopcocks, the other two with sealed tubes, in order to assure ourselves that we located the critical mixing point within the limits of our experiments.

Phase-Separation Temperature Measurements. Temperatures of phase separation were measured in an insulated constant-temperature bath, usually cooling at a rate of 0.001°/min. A calibrated Beckman thermometer, a VECO thermistor with a Wheatstone bridge, and a NBS calibrated Leeds and Northrup 8163 platinum resistance thermometer with a L and N 8069 Type G-2 Mueller bridge and a L and N 2285B Type HS galvanometer were used for temperature measurements. Although we have measured our phase-separation temperatures to 0.001°, we want to stress that our conclusions would remain valid even if we had determined our temperatures to 0.01°.

Light-Scattering Photometry. Detailed description of the light-scattering photometer has been given elsewhere.[2,4,14] Only the changes will be specified. The cell holder and the detector slit system are mounted on adjustable mechanical stages. The easier alignment procedure enables us to extend our angular range from 11 to 140°. Temperature of the thermostat bath was controlled to 0.001°.

Laser Homodyne "Self-Beating" Spectrometer. Our laser spectrometer has been described elsewhere.[13,15] We have, in essence, used three different types of He–Ne CW gas lasers: a radiofrequency–direct current excited laser with an output power of 70 mW (Spectra Physics Model 125),[13] a radiofrequency excited laser with an output power of 5 mW (Spectra Physics Model 115),[15] and a dc-excited laser with an output power of 20 mW (Spectra Physics Model 124). The main portion of the work has been performed using the dc-excited laser. The load resistor,[15] R_L, can be varied from 1 to 50 kohms depending upon the frequency range which we want to investigate. The signal-to-noise ratio of the output signal from our analog squarer[15] has been improved using a Varian C-1024 time-averaging computer by repeated scans instead of one slow scan with a low-pass filter. The constant-temperature bath in the laser spectrometer was controlled to ±0.001°. Temperature drift was less than 0.005° over a 24-hr period. Temperature gradients less than 0.04° were found in the oil bath (3-gal capacity), so we introduced a 5-mm thick copper block around the sample cell to ensure uniformity of temperature over the whole fluid mixture. The phase-separation temperature of the samples was measured (a) in a separate insulated bath, (b) inside the light-scattering photometer, and (c) inside the laser spectrometer. The observed phase-separation temperatures agree to within 0.02° over an 18-month period in terms of absolute determination of temperature. For temperature distances $\Delta T = T - T_c$ used in this experiment, we have an error less than 0.005°. We measured the heating of an oil-filled sample cell by the dc-excited laser at full power (20 mW) with a thermistor located just above the beam path. Temperature increases of about 0.003° could be observed. To avoid this uncontrollable heating effect during our measurements at $\Delta T < 0.2°$, we reduced the incident light intensity by dark neutral filters with a transmittance of $^1/_{20}$ and $^1/_{200}$, respectively.

Results and Discussion

Coexistence Curve. Our coexistence curve, as shown in Figure 1, is not comparable to the work of Thompson and Rice,[16] on the system perfluoromethylcyclohexane–carbon tetrachloride, but approaches the precision of the work on the system aniline–cyclohexane.[17] We may use the cubic relation to try to locate the critical solution concentration, as shown in Figure 2. The critical mixing point (38.8 wt % isobutyric acid in water, maximum phase-separation temperature 26.12°) was in fair agreement with the best in the literature.[18] We should, however, mention that we discarded two samples (represented by solid circles in Figure 1 at concentration 39.0 and 39.9 wt %) for the cubic plot in Figure 2 because both samples had their phase-separation temperatures off by about 0.03°. Our measurements showed that the coexistence curve appears to follow a cubic relation to within a few thousandth degree of the critical solution temperature. It was also possible to fit the coexistence curve by using a relation $(\Delta T)^\delta = \mathcal{C}(C - C_0)$ with δ being the exponent, not necessarily equal to $^1/_3$, and C_0 the critical solution concentration. Then, $\ln(\Delta T) = 1/\delta \ln(C - C_0) + \ln \mathcal{C}^{1/\delta}$ so that variations in δ could be estimated from variations in T_c and C_0 by the least-squares method. The value of $^1/_3$ for δ was consistent with Figure 2.

Angular Dependence of Scattered Intensity. The angular dependence of scattered intensity for the critical mixture isobutyric acid and water was first investigated by Chow.[19] We expected the scattering behavior to obey the Ornstein–Zernike and Debye theory of critical opalescence, as shown in Figure 3. Measurements with λ_0 = 365, 436, 578, and 632.8 mμ give normal behavior. At larger temperature distances, the system has low scattered intensity and, therefore, it is faintly opalescent. Then dust and stray light become more important. For example, the small downward dip at small values of the scattering angle in Figure 3 is caused by the very strong forward scattering of dust particles. We have intentionally avoided studies in the immediate neighborhood of the critical mixing point because of multiple scattering. Our aim here is to utilize the existing knowledge on angular dissym-

(14) B. Chu, *Rev. Sci. Instr.*, **35**, 1201 (1964).

(15) B. Chu, *J. Chem. Phys.*, **47**, 3816 (1967).

Note: In this reference, we have defined that, according to Fixman,[9] $a = D(\partial\pi/\partial c)_T$ in which D is called a diffusion constant. The usual definition for the mutual diffusion coefficient is $D(\partial\pi/\partial c)_T$ which includes the $(\partial\pi/\partial c)_T$ term. In this article, we have changed our notation as suggested by Paul Martin, Harvard University, to $a = D = \alpha^*(\partial\pi/\partial c)_T$ in which α^* is the transport coefficient and D is the mutual diffusion coefficient.

Ref 15	This article
a	a
D	α^*
$D(\partial\pi/\partial c)_T$	D

(16) D. R. Thompson and O. K. Rice, *J. Am. Chem. Soc.*, **86**, 3547 (1964).

(17) D. Atack and O. K. Rice, *J. Chem. Phys.*, **22**, 382 (1954); O. K. Rice, *ibid.*, **23**, 164 (1955).

(18) D. Woermann, *Bunsengesellschaft*, **69**, 319 (1965).

(19) Q. Chow, *Proc. Roy. Soc.* (London), **A224**, 90 (1954).

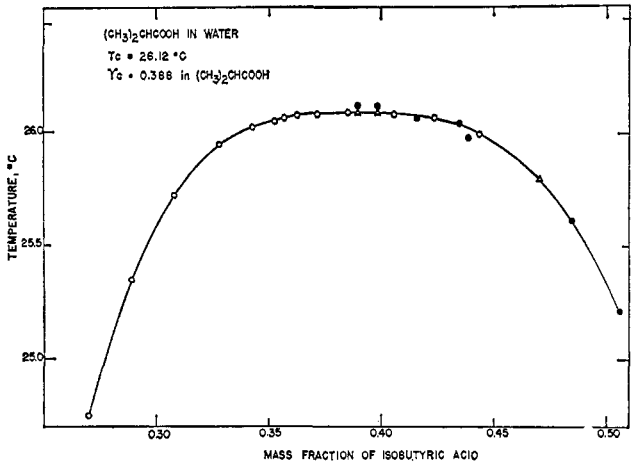

Figure 1. Plot of phase-separation temperature *vs.* mass fraction of isobutyric acid. Hollow and solid circles represent two separate sets of samples prepared in sealed glass tubes. Hollow triangles represent samples prepared in cells fitted with Teflon stopcocks.

metry and coexistence curve so that we may put ourselves on a more solid foundation for later discussions.

According to the Debye theory,[3] eq 1 may be represented in another form as

$$\frac{1}{I_{c,\theta}^*} = F(T)\left(\frac{T_c}{T}\right)\left[\frac{\Delta T}{T_c} + \frac{8\pi^2}{3} l^2 \frac{\sin^2(\theta/2)}{\lambda^2}\right] = A + B\sin^2\frac{\theta}{2} \quad (5)$$

where $I_{c,\theta}^*$ is the relative scattered intensity due to concentration fluctuations at angle θ; $F(T)$ is a temperature function for attenuation correction; l is a Debye molecular interaction parameter. We recall[4] that (a) the measured scattered intensity has a small contribution due to density fluctuations which may depend upon the interaction between the two components, and (b) the temperature dependence of reciprocal zero-angle extrapolated scattered intensity may not necessarily follow eq 5, although the form of eq 5 suggests how we can proceed to obtain this dependence. We have argued against the presence of *very* long-range correlations in our temperature range and feel that measurements down to $\theta = 11°$ are sufficiently close to 0° for us to make a meaningful extrapolation to zero angle. Figure 4 shows a plot of A/B *vs.* $(T - T_c)$. We use A/B to avoid determining $F(T)$ since we may write

$$\frac{A}{B} = \left(\frac{3\lambda^2}{8\pi^2 l^2}\right)\left(\frac{T - T_c}{T_c}\right)^{\gamma} \quad (6)$$

In the Debye theory, $\gamma = 1$. In our experimental determination of the temperature dependence of reciprocal extrapolated zero-angle scattered intensity, deviation from the linear behavior in Figure 4 tells us $\gamma \neq 1$. We have checked our results using two separate samples, measuring one sample at two different times, and finally using two light-scattering photometers of different optical geometry[4,13-15] and with different wavelengths (λ_0 = 436, 578, 632.8 mμ). Figure 5 shows a plot of log A/B *vs.* log $(T - T_c)$. We note that $\gamma > 1$. In order to determine γ we should recall point a. For a relatively weak opalescent system, the background correction due to density fluctuations becomes important

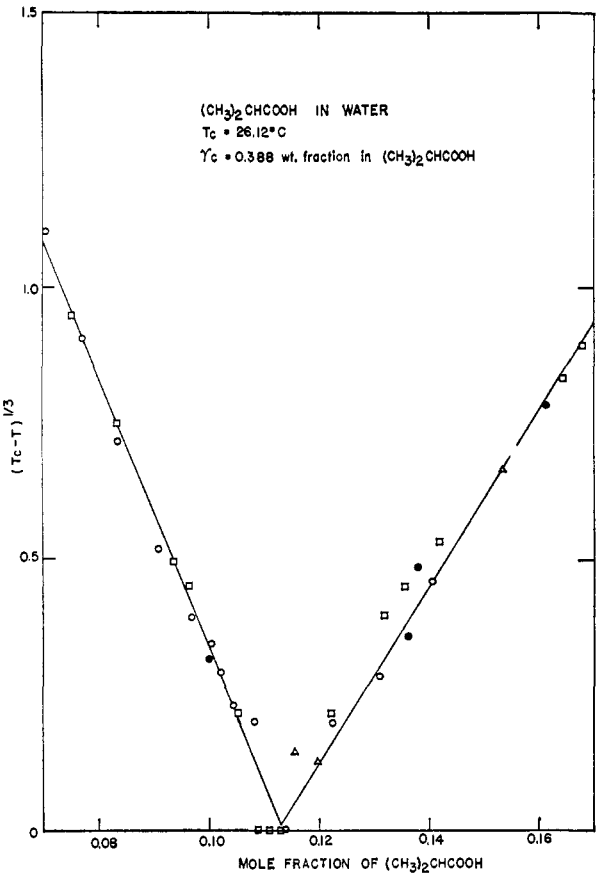

Figure 2. Plot of $(T_c - T)^{1/3}$ *vs.* mole fraction of isobutyric acid. The symbols are the same as in Figure 1. Hollow squares represent the data of Woermann[18] with T_c = 26.30°.

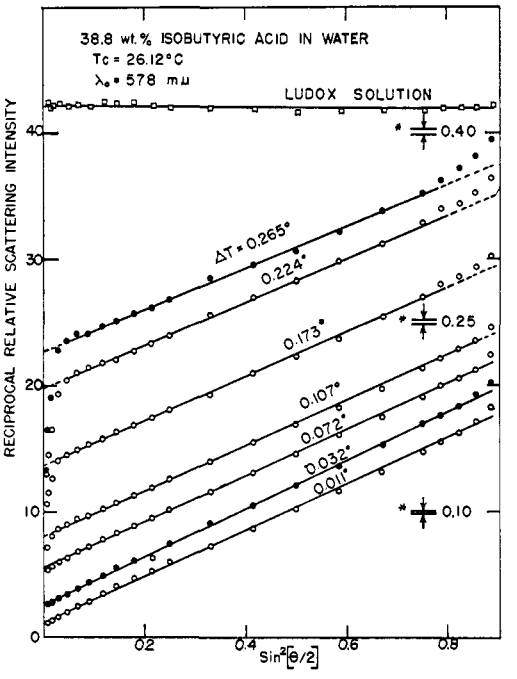

Figure 3. Plot of reciprocal relative scattered intensity *vs.* $\sin^2(\theta/2)$. Angular range 11–140°. Hollow and solid circles represent measurements from the sample I but 14 days apart. * designates 1% spread.

when ΔT gets larger. The dotted line in Figures 4 and 5 represents estimates of A/B after density and dust corrections. We have used the scattered intensity mea-

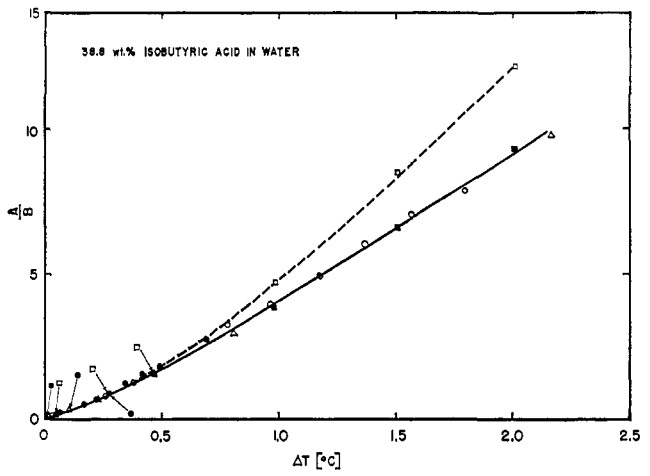

Figure 4. Plot of A/B *vs.* $(T - T_c)$. All measurements have been reduced to $\lambda_0 = 436$ mμ. Hollow and solid circles represent measurements from sample I but 14 days apart. Hollow triangles represent data from sample II. Hollow and solid squares represent measurements from a He–Ne CW gas laser ($\lambda_0 = 6328$ Å) with sample I. Solid line corresponds to data without correction. Dotted line corresponds to data with correction.

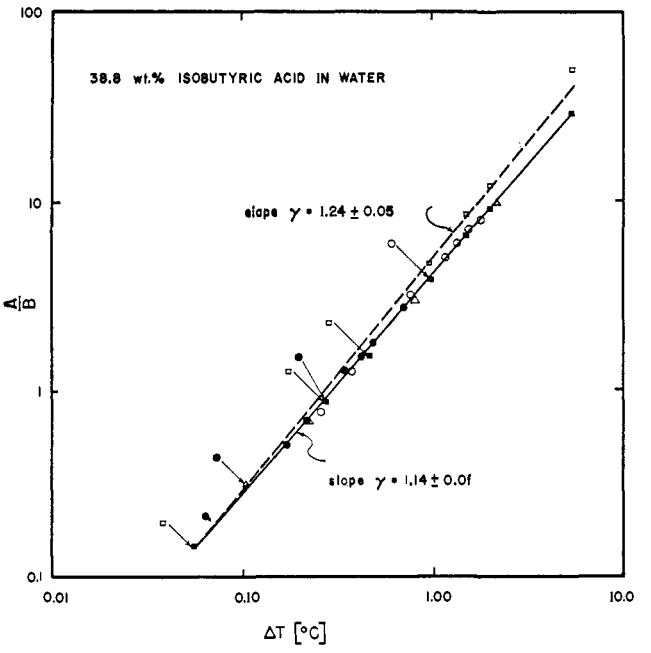

Figure 5. Plot of log (A/B) *vs.* log $(T - T_c)$. The symbols are the same as in Figure 4.

sured at $\Delta T = 16.76°$ as the upper limit of contributions due to density fluctuations (Figure 6). It should be noted that any form of pure density correction on A/B decreases the value of γ. We have obtained $\gamma = 1.24$ using the scattered intensity measured at $\Delta T = 16.76°$ as background. Conversely, if we use the measured scattered intensity, which contains a small portion of the light due to density fluctuations and dust without background correction, it will give us a different γ. In our case, γ (without correction) $= 1.14 \pm 0.01$ and γ (with correction) $= 1.24 \pm 0.05$ and the true γ is probably very near 1.24 rather than 1.14. In any case, the correct γ should be between the two limits. We may relate the temperature

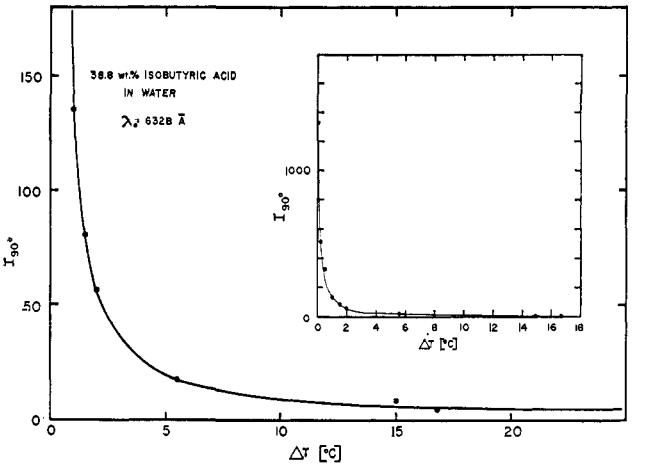

Figure 6. Plot of relative scattered intensity at 90° *vs.* $(T - T_c)$. $\lambda_0 = 632.8$ mμ.

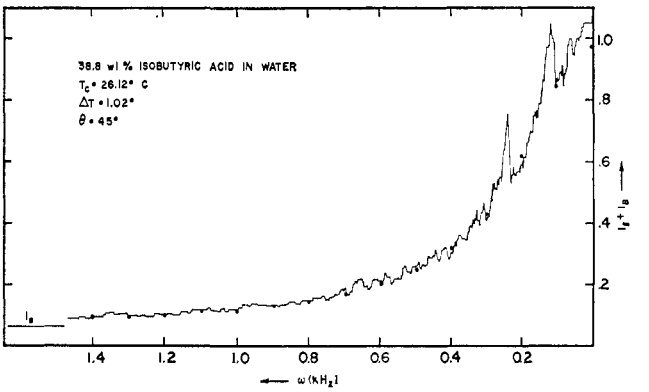

Figure 7. Power spectrum of the scattered light at $\theta = 45°$ by 38.8 wt % isobutyric acid in water at $T - T_c = 1.02°$. The solid circles represent a Lorentzian line of 0.25-kHz half-width ($=2\Gamma$). Noise was damped by a 3-sec time constant and by averaging six $I(\omega)$ scans with a computer averager.

dependence of A/B to $(\partial\pi/\partial c)_T$ as

$$\lim_{K\to 0} \frac{1}{I_c^*} \propto \left(\frac{A}{B}\right) \propto \left(\frac{\partial \pi}{\partial c}\right)_T \propto (T - T_c)^{\gamma} \qquad (7)$$

It is perhaps noteworthy that the value of γ ($=1.24 \pm 0.05$) is very close to the value of $^5/_4$, which is determined from a three-dimensional Ising model.

Line-Width Studies. Preliminary results on line-width studies of the isobutyric acid–water system have been reported elsewhere.[13,15] It has been shown[13,15] that (a) the power spectrum is a Lorentzian-shaped line, (b) $\Gamma = aK^2$ holds whenever the magnitude of correlation is small, (c) Γ approaches zero as K approaches zero, and (d) eq 4 is a good approximation in the neighborhood of the critical point where long-range correlations are important. Figure 7 shows a typical power spectrum ($I_S + I_B$) for the isobutyric acid–water system at $\Delta T = 1.02°$ and $\theta = 45°$. The solid circles represent a calculated Lorentzian line using the equation

$$1/I_S = A^* + B^*\omega^2 = 1.10 + 18.1\omega^2 \quad (\omega \text{ in kHz})$$

where $A^*/B^* = (2\Gamma)^2$. Figure 8 shows a plot of $1/I_S$ *vs.* ω^2. The error limits in the plot are the maximal uncertainties given by the recorded power spectrum and the background. For a typical plot with 15 curve

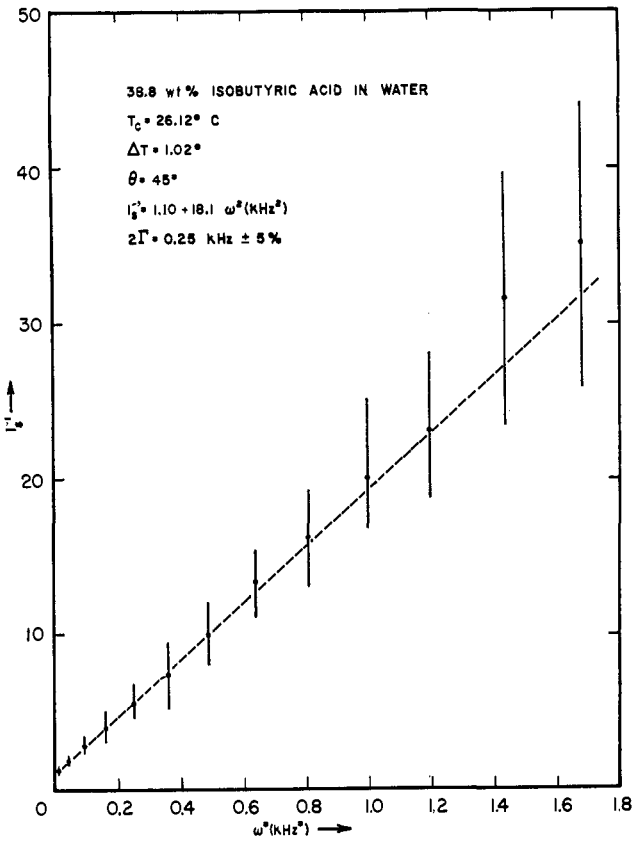

Figure 8. Plot of the reciprocal of the power output (I_S in Figure 7) *vs.* ω^2. The error limits are the maximal uncertainties given by the recorded power spectrum and the background correction.

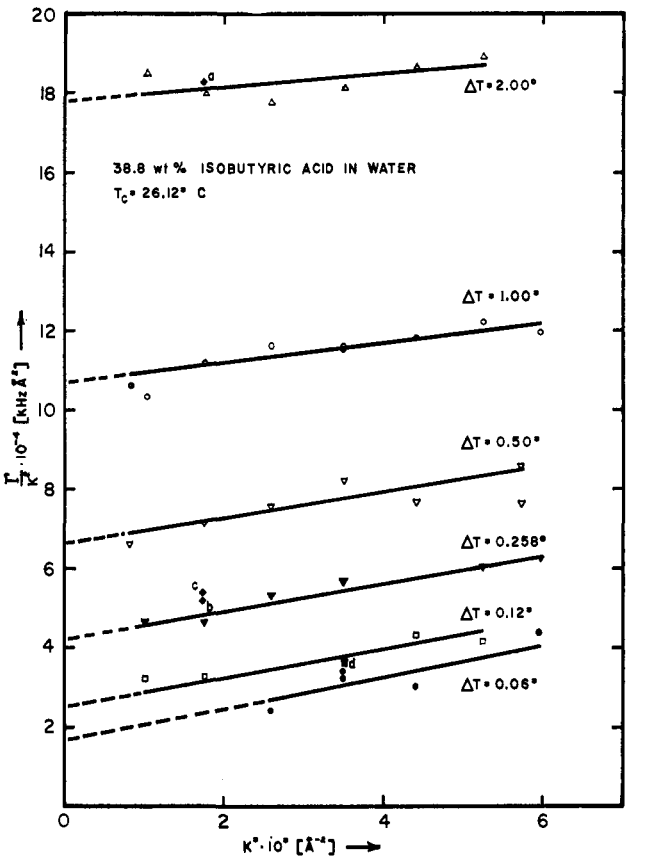

Figure 9. Plot of Γ/K^2 *vs.* K^2. Points a–d represent data obtained with sample II, all others sample I. Point c was obtained by turning the polarization direction of the laser beam which was originally perpendicular to the plane of observation by 90°. Point d shows that there is no influence due to heating of the sample cell by the intense incident laser beam in our temperature range because we have obtained the same result using either < 1 or ~ 18 mW.

points, the over-all limit of error for the line-width determination is less than ±5%. Figure 9 shows a plot of Γ/K^2 *vs.* K^2. The slight slope in the Γ/K^2 dependence of K^2 for each ΔT undoubtedly comfirms the existence of a K^4 term as expressed in eq 4. Although all points in Figure 9 represent measurements of only one sample, we could reproduce these values with another sample of the same concentration. Furthermore, we found the same line widths within the above-mentioned error range by changing the power of the incident laser light from 20 to 1 mW at $\Delta T = 0.12°$ and also by turning the polarization direction of the laser beam which was originally perpendicular to the plane of observation by 90°. Figure 9 allows us to extrapolate the Γ/K^2 values to zero angle and provides us an estimate on a ($\equiv D$) at different temperatures. By definition, we have

$$a \equiv \lim_{K \to 0} \frac{\Gamma}{K^2} = \alpha^* \left(\frac{\partial \pi}{\partial c}\right)_T$$

Figure 10 shows a plot of $\log a$ *vs.* $\log (T - T_c)$. With

$$a = \alpha^* \left(\frac{\partial \pi}{\partial c}\right)_T = \text{constant} \times (T - T_c)^{\gamma^*} \qquad (8)$$

we find $\gamma^* = 0.68 \pm 0.04$. If the transport coefficient, α^*, were insensitive to the temperature distance from the critical solution temperature, as has often been assumed, we would find $\gamma = \gamma^*$ according to eq 7 and 8. Instead, we have found that $\gamma \neq \gamma^*$.

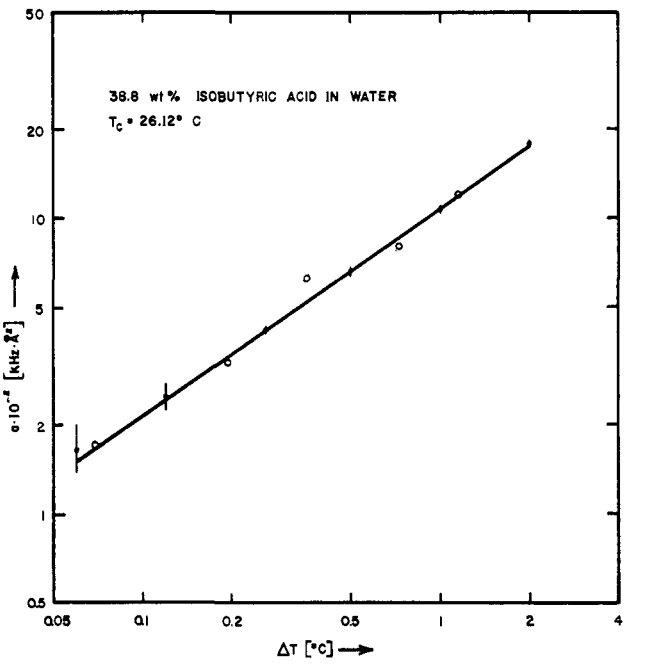

Figure 10. Plot of $\log a$ *vs.* $\log (T - T_c)$. $a = \lim_{K \to 0} \Gamma/K^2$. $\gamma^* = 0.68 \pm 0.04$. The solid circles represent line-width studies using a Spectra Physics Model 115 radiofrequency excited He–Ne laser.[15] Filled circles represent line-width studies using a Spectra Physics Model 124 dc-excited He–Ne laser.

Summary and Conclusion

Before we analyze γ and γ^*, let us summarize what we have done experimentally. We have (1) purified

both components to the limits of present-day techniques; (2) estimated the presence of impurities in isobutyric acid by gas chromatography with different columns; (3) redetermined the coexistence curve using samples with different sealing techniques; (4) ascertained the stability of the system by reproducing phase-separation temperatures over a several months period; (5) avoided multiple scattering and gravitational effects by staying away from the very immediate neighborhood of the critical point; (6) reproduced our results using two separately prepared samples at the critical solution concentration; (7) ensured uniformity of temperature in the scattering cell by means of a massive copper shield; (8) studied the angular dissymmetry with visible light of different wavelengths and with different optical geometry, (9) used lasers excited by radio-frequency, direct current, and radiofrequency–direct current; (10) checked the frequency response of the spectrometer, the pick-up, vibration, and background problems; (11) calibrated the linearity of the analog squarer; (12) reduced the signal-to-noise ratio by means of a time-averaging computer, or a low pass filter; (13) examined the heating effect of the higher powered lasers, and (14) minimized the effects of stray light and reflections in our scattering measurements. We worried about the effects of depolarization and rotational contributions because of the complexities of our molecules. So we tried to measure the line width at $\theta = 90°$ with laser light polarized parallel to the direction of observation. Only a broad background was observed at $\Delta T = 0.5°$. We then checked the depolarization by inserting an analyzer in our light-scattering photometer at $\Delta T \sim 0.1°$. We found that the amount of depolarized light was about a few per cent, insufficient to account for any significant rotational contribution. What does $\gamma^* \approx {}^2/_3$ and $\gamma \approx {}^5/_4$ imply? If we take $(\partial\pi/\partial c)_T \propto (T - T_c)^{\gamma}$ and $\alpha^*(\partial\pi/\partial c)_T \propto (T - T_c)^{\gamma^*}$, we find for $T > T_c$, $\alpha^* \propto (T - T_c)^{\gamma^* - \gamma}$ with $\gamma^* - \gamma < 0$. This means that α^* has to increase as T approaches T_c. The self-diffusion coefficient decreases with increasing viscosity and the viscosity increases as T approaches T_c. The product, $\alpha^*(\partial\pi/\partial c)_T$, behaves within reason since it approaches zero as $T \rightarrow T_c$.

The discrepancy ($\gamma \neq \gamma^*$) in our light intensity and line-width studies implies that the transport coefficient α^* diverges as $(T - T_c)^{\gamma^* - \gamma}$ within the temperature range of our investigation.

Acknowledgment. One of us (B. C.) wishes to thank Professor Paul C. Martin of the Harvard Physics Department for some very helpful comments.

Translational Diffusion Constant of Polymer Chains[1a]

Arturo Horta[1b] and Marshall Fixman

Contribution from the Department of Chemistry, Yale University, New Haven, Connecticut 06520. *Received November 21, 1967*

Abstract: The formal theory of the translational diffusion constant is reexamined in order to display in isolation the contributions from (a) the equilibrium average derived by Kirkwood, and (b) corrections due to distortion of the equilibrium segment distribution. The corrections are found to be small in good or poor solvents. The equilibrium contribution requires a calculation of $\langle 1/r_{ij} \rangle_{eq}$ for all pairs of segments i and j in the chain, and this calculation has been carried through on the basis of a boson operator formalism recently introduced. It is first shown that the boson formalism in lowest order gives a Gaussian distribution of r_{ij}, with a variance dependent on i and j and on the magnitude of the excluded volume. A calculation of the frictional expansion factor α_f shows that it increases much less rapidly with increasing goodness of solvent than other measures of chain dimension. However, the tentative conclusion is expressed that this behavior of α_f is due to the sensitivity of $\langle 1/r_{ij} \rangle_{eq}$ to non-Gaussian statistics, in comparison with $\langle r_{ij} \rangle^2$. Methods for dealing with this sensitivity are outlined.

I. Introduction

The translational diffusion constant is conceptually the simplest transport coefficient of chain polymer molecules, and was one of the first to be investigated. Kirkwood[2] presented for the diffusion constant an expression involving just equilibrium averages of the reciprocal distances between segments. His expression was first regarded as exact but was later shown to be approximate, the corrections being identified by Ikeda[3] and Erpenbeck[4] (see also Saito[5]). Our goals here are two: (1) to present explicitly the (small) correction to Kirkwood's formula and to examine the dependence of the correction on excluded volume forces; (2) to calculate the effect of excluded volume on the diffusion constants as given by Kirkwood's formula.

Regarding the first goal, the magnitude of the correction can be gauged in several ways, for example, by exact calculation for particular systems. Zwanzig[6] has pointed out that the rigid ring has a diffusion constant smaller by the ratio 11/12 than that calculated from Kirkwood's formula. Approximate calculations are required for chain polymers, and our results, which reduce to those of Zimm[7] at the θ temperature, indicate a

(1) (a) Supported in part by National Institutes of Health Research Grant GM 13556-03. (b) Fellow of Fundación Juan March.

(2) J. G. Kirkwood, *Rec. Trav. Chim.*, 68, 649 (1949); (b) *J. Polymer Sci.*, 12, 1 (1954).

(3) Y. Ikeda, *Kobayashi Rigaku Kenkyusho Hokoku*, 6, 44 (1956).

(4) J. J. Erpenbeck and J. G. Kirkwood, *J. Chem. Phys.*, 38, 1023 (1963).

(5) N. Saito, K. Okano, S. Iwayanagi, and T. Hideshima, *Solid State Phys.*, 14, 343 (1963).

(6) R. Zwanzig, *J. Chem. Phys.*, 45, 1858 (1966).

(7) B. H. Zimm, *ibid.*, 24, 269 (1956).